Swiss Accelerator Research and Technology

CHART Scientific Report (Final Report for Phase 2)

Mechanical Modelling and Failure Identification of Nb_3Sn Rutherford cable stacks

(MagComp)

ETHZ:
Dr. Xiang Kong, Prof. Dr. Theo Tervoort

PSI:
Dr. Bernhard Auchmann, Dr. André Brem, Dr. Araujo, D.M.

29.07.2024

1. Introduction / Original goals of this project

The aim of this research project is to develop a comprehensive anisotropic mechanical model of Nb_3Sn Rutherford cable stacks and examine their failure modes by monitoring deformation processes using techniques such as digital image correlation (DIC). These experimental results will be cast into a constitutive equation that characterizes the anisotropic finite-strain mechanical behaviour of the cable stacks for application in finite element modelling. This project is in collaboration with the Superconducting Magnets Group of PSI, where the cable stacks will be produced.

To explore the role of the matrix material's fracture toughness, we will use both a brittle epoxy and a tough epoxy, as well as a wax system for impregnating the coils. The brittle epoxy will be a standard commercial product used in cryogenic applications, while the tough epoxy is being developed in the CHART2 project. The wax material will be selected in collaboration with the Superconducting Magnets Group of PSI.

In the CHART1 project, a collaboration between CERN, PSI, and ETHZ, experimental techniques were developed to characterize the thermo-mechanical behaviour of epoxy systems and applied to four commercially used epoxy systems in superconductive magnets. In CHART2, new epoxy systems are being designed to combine a high fracture toughness with low viscosity and long pot life, essential for producing Nb_3Sn Rutherford cable stacks.

This research proposal aims to build on the results from CHART1 and CHART2 by investigating the impact of these newly developed epoxy systems on the mechanical behaviour of Nb3Sn

Rutherford cable stacks. Providing detailed constitutive equations for the mechanical behaviour of cable stacks is expected to facilitate efficient magnet manufacturing.

2. Realisation

The Nb_3Sn Rutherford cable stacks, referred to as 10-stack cables, exhibit a multiscale structure as depicted in Fig. 1. Each stack consists of 10 cables, with 20 strands per stack. At the cubic level, around 15 mm in size, the structure includes the superconductive strands, fiberglass insulation layers, epoxy resin for impregnation, and steel films. At the single strand level, with a submicron diameter, each strand comprises an outside layer and a core consisting of annealed copper and microfilaments. The microfilament section features superconducting Nb_3Sn filaments approximately 50 micrometers in diameter, embedded in a copper matrix.

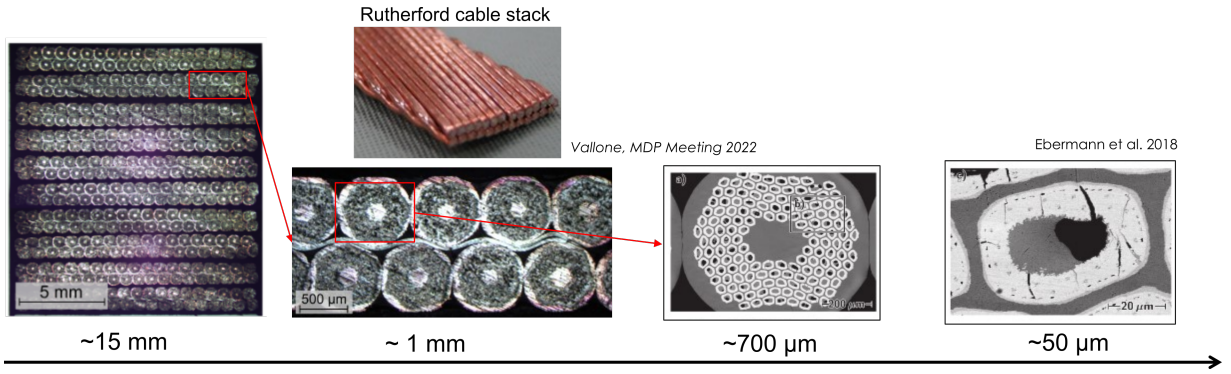

Figure 1: Multiscale structure of 10-stack Rutherford cable stacks from cubic level (~15mm), stack level (1 mm), single strand down to Nb_3Sn micro filaments in 50 micrometres[1].

A non-contact, image-based *in situ* measurement was developed for 10-stack uniaxial compression testing. This method provides not only a 2-point macroscopic measurement, represented by the blue square in Fig. 2(c), acting as a visual extensometer especially at low temperatures, but also strain fields of the entire sample through digital image correlation (DIC). Additionally, tracking strand-cores by a particle-tracking method allows for a more detailed understanding of the strain-damage mechanism.

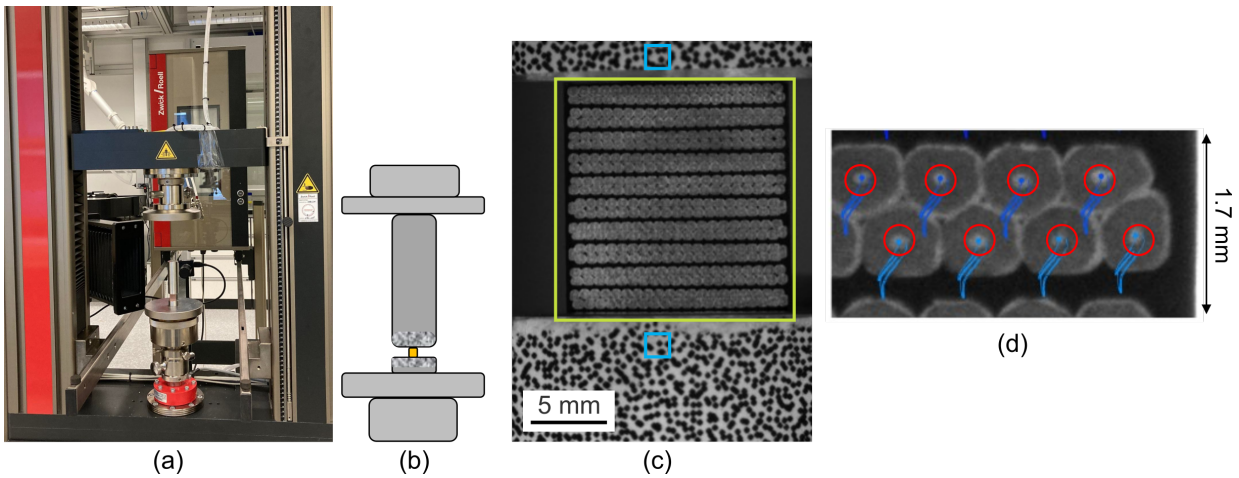

Figure 2: (a) Universal testing machine equipped with a synchronized camera focussed on the 10-stack surface. (b) Schematic of the uniaxial compression set-up, showing the 10-stack cable stacks in yellow, loaded by steel rods with speckles to capture the image stack. (c) Image stack at cubic level and (d) the trajectory of strand-cores (blue) by a particle tracking method during the compression test.

The mechanical properties of epoxy resins are highly temperature- and strain rate-dependent[2]. Fig. 3 (a) presents a graphical overview of the performed experiments in a map of strain rate (10^{-4} to 10^{3} s^{-1}) versus temperature (77 to 353K). The experimental data (coloured dots) are collected using a universal testing machine equipped with (b) a temperature chamber, (c) cryogenic set-ups as well as (d) a split Hopkinson pressure bar for dynamic testing.

Cryogenic experiments were performed with ① specimens (see Fig. 3b for the numbered items) fully immersed in a liquid nitrogen LN_2 (-196 ˚C=77 K) bath. The home-build setup consists of ② two cylindrical steel rods, ③ an aluminium container, ④ a ceramic brick and ⑤ a centre hole plate 3D printed in polyethylene terephthalate (PET) as demonstrated in Fig.3 (c). The ceramic brick ④ was placed between the container and the bottom platen for thermal insulation to avoid affecting the load cell. The centre hole plate is used to align the bottom rod.

A classical split Hopkinson pressure bar (SHPB) facilitates dynamic experiments at initial speeds up to several meters per second. The system primarily comprises a striker, an input bar, an output bar, and a gas gun as the launching system, as depicted in Fig. 3(d). For cold temperature tests, samples are first cooled in a polystyrene box filled with solid carbon dioxide (dry ice) and then transferred to a climatic chamber, also containing dry ice, before testing.

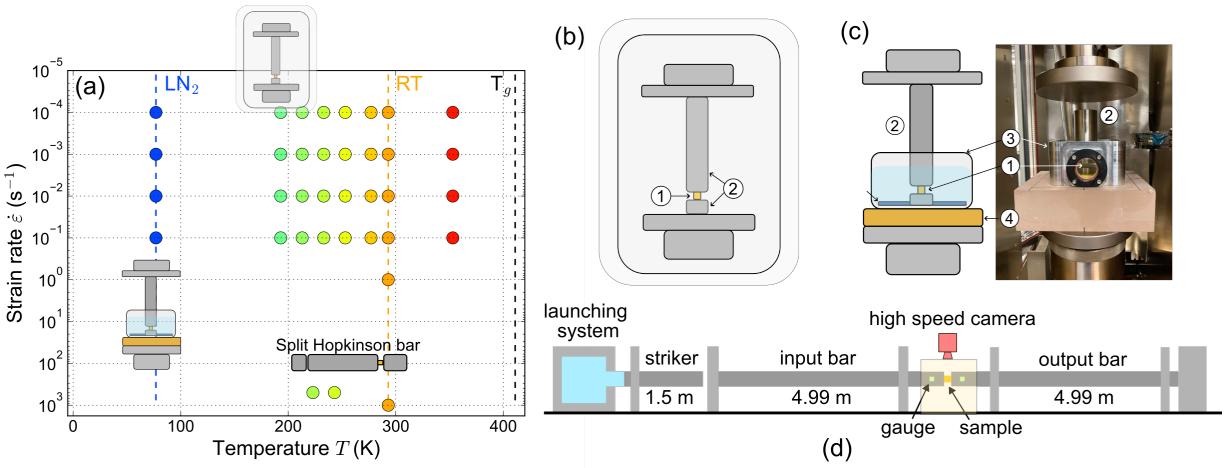

Figure 3: (a) An overview of the performed experiments (as dot) in the map of strain rate and temperature. (b) schematics of uniaxial compression test on a cylinder sample in a thermos chamber (193K-353K); (c) schematics of uniaxial compression on a sample totally immersed in the liquid nitrogen (LN2) bath. (d) Schematic of split Hopkinson pressure bar system to achieve dynamic compressive test at 10^{3} s^{-1} strain rate level.

Numerically, a simplified 2D mesh of 10-stack cables is designed in Fig.6 for the computation simulations via finite element software Ansys APDL.

3. Results / Conclusions / Deliverables

3.1 Experimental measurement vs. numerical simulation of Nb_3Sn 10-stack cables

The curve in terms of nominal stress - engineering strain is shown in Fig. 4 (a) measured using different techniques. These are digital image correlation (DIC), an extensometer and corrected displacement of machine crosshead respectively. The strain field obtained by DIC reveals strain localization on the glass fiber insulation layer and between two stacks. The experimental results are compared to the numerical finite element simulations as shown in (c).

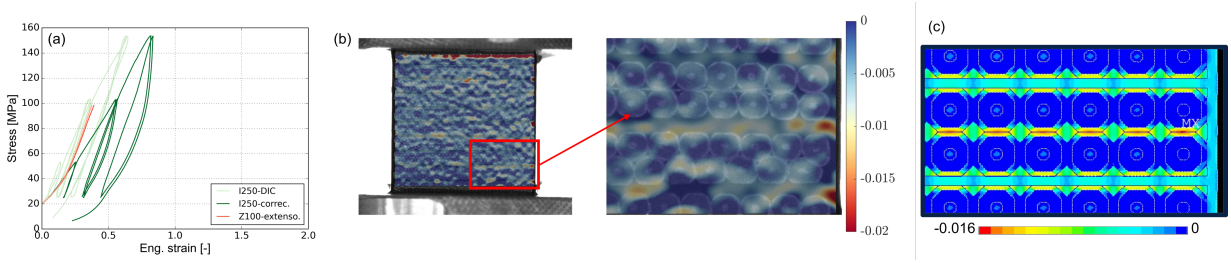

Figure 4: (a) nominal stress – engineering strain curves of 10-stack cable stacks measured by different methods. (b) Strain field by digital image correlation (DIC) in comparison to the results by finite element computation.

3.2 Components characterization

Characterization of each component in a 10-stack cable is necessary to better understand the mechanical properties and to simulate the sample as a composite representative volume element cube.

The resin used was a standard commercial epoxy grade, CTD101K. The mechanical properties of this epoxy resin, used to impregnate the cable stacks, are strongly temperature- and strain rate-dependent. The experimental values of the yield stress as a function of (a) strain rate and (b) temperature, are depicted in Fig. 5. As can be seen in this figure, the Ree-Eyring equation with only 6 parameters is able to fit the experimental yield stress data over a wide range of temperatures and strain rates. The model predicts that the yield stress extrapolated to 0 K for different strain rates, converges to 569 MPa (red star in Fig. 5b). According to the Ree-Eyring model, the strain-rate dependence of the yield stress decreases with decreasing temperature and is predicted to vanish as the temperature approaches T = 0 K.

A 3D presentation of the yield-stress surface as a function of strain rate and temperature is shown in (c). For certain temperatures, the yield stress as a function of the logarithmic strain rate depicts a curve with two slopes (see Fig. 5a), a low slope representative of the α-process (the glass transition) at elevated temperatures and a higher slope due to the α + β processes at low temperatures. In the α-region, the β-process contribution can be neglected. The β-process is a so-called “secondary transition”, typically due to the activation of motion of a side group or part of the main chain of the polymer. It plays a role at low temperatures or high strain rates, below the so-called “β transition”. The β-temperature transition point shifts to a higher value upon increasing strain rate.

A thermo-rheological complex constitutive model based on the reduced time approach, using stress- and temperature-shift factors for each process, was successfully applied to describe the full nonlinear viscoelastic behavior of the epoxy resin up to the yield point[3].

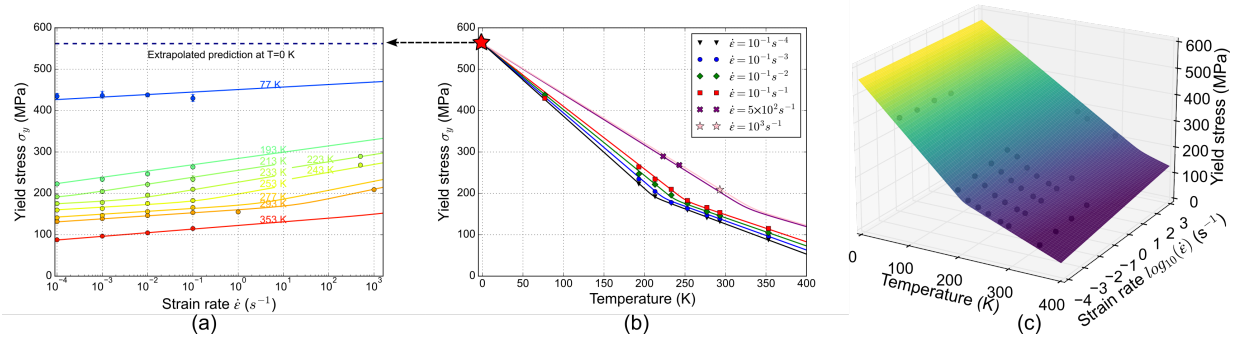

Figure 5: Ree-Eyring equation fitting on yield stress from experimental results performed at different conditions. The yield stress evolution in terms of (a) strain rate and (b) temperature. (c) A surface of yield stress-strain rate-temperature obtained by Ree-Eyring equation compared with experimental data (as black dot).

The other components that make up a Rutherford cable were found to have mechanical properties that are much less dependent on temperature and strain rate, going from room temperature to liquid nitrogen. The yield stress of annealed copper was measured and found to be less than 20 MPa, which is relatively low compared to the other components. A Voce isotropic hardening constitutive equation was successfully used to model non-linear hardening behavior for annealed copper up to 10% strain.

As for the fibre glass insulation layer and superconductive Nb_3Sn phase, they are generally assumed to behave as Hookean elastic materials with a high yield stress of more than 250 MPa and 400 MPa, respectively[4,5], and were used as such in our finite element simulations.

3.3 Numerical finite element simulation using a simplified 2D octagon geometry

After characterizing the mechanical behavior of each component, it became evident that the annealed copper phase plays a major role in the 10-stack cables due to its low yield stress. This indicates that the geometry of the copper strand layer significantly affects the global stress-strain response. Finite element calculations using different strand-layer geometries, with the ratio of superconducting phase to strand diameter varying from 0.77 to 0.95, indeed exhibit strongly different global stress responses.

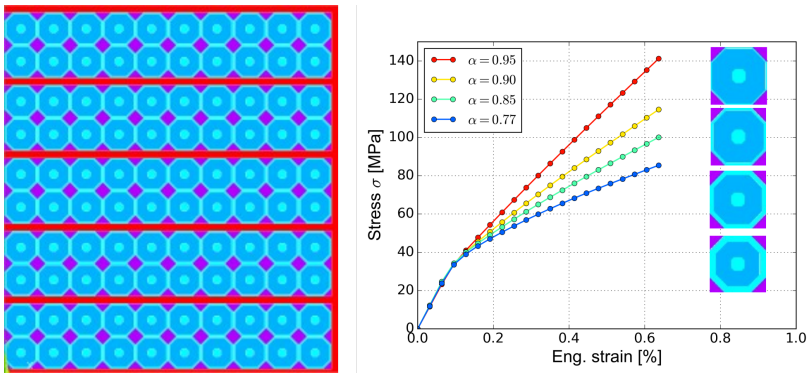

Figure 6: (a) A simplified 2D octagon geometry simulated as a quarter of 10-stack cables. (b) Nominal stress - engineering strain curve from strand geometry with different copper layer thickness.

4. Publications and Outreach

- Kong, X.; Tervoort, T.A.; Brem, A.; Araujo, D. M.; Auchmann, B.; Mechanical identification and modelling of impregnated Nb3Sn Rutherford cable stacks under compressive loading, **2024**, 19th European Mechanics of Materials Conference (EMMC19), Madrid, Spain.
- Kong, X.; Tervoort, T.A.; Brem, A.; Araujo, D. M.; Auchmann, B.; Mechanical identification and modelling of impregnated Nb3Sn Rutherford cable stacks under compressive loading, **2024**, 19th Conference on Deformation, Yield and Fracture of Polymers, Kerkrade, the Netherlands.
- Studer, P.; Kong, X.; Tervoort, T.A.; Brem, A.; Araujo, D. M.; Auchmann, B.; Determination of deformation via image-based measurements and design of epoxy systems for Nb3Sn Rutherford cables. **2023**, HFM annual meeting, CERN Geneva Switzerland.
- Kong, X.; Tervoort, T. A.; Govaert, L.; Li, X.Y.; Grolleau V. Modeling of temperature- and rate-dependent mechanical behaviors: Application to the characterization of an epoxy resin system from room to cryogenic temperatures, in preparation.

5. References

(1) Ebermann et al. 2018, *Irreversible degradation of Nb_3Sn Rutherford cables due to transverse compressive stress at room temperature*, Supercond. Sci. Technol. 31 (2018) 065009

(2) André Brem, Barbara J. Gold, Bernhard Auchmann, Davide Tommasini, Theo A. Tervoort, *Elasticity, plasticity and fracture toughness at ambient and cryogenic temperatures of epoxy systems used for the impregnation of high-field superconducting magnets*, Cryogenics, Volume 115, (2021), 103260

(3) Kong, X.; Tervoort, T. A.; Govaert, L.; Li, X.Y.; Grolleau V. Modeling of temperature- and rate-dependent mechanical behavior of polymer glasses: Application to the characterization of an epoxy resin system from room to cryogenic temperatures, in preparation.

(4) C. Scheuerlein, F. Lackner, F. Savary, B. Rehmer, M. Finn and P. Uhlemann, "*Mechanical Properties of the HL-LHC 11 T Nb3Sn Magnet Constituent Materials*," in IEEE Transactions on Applied Superconductivity, vol. 27, no. 4, pp. 1-7, (2017), 4003007

(5) M. Daly *et al.*, "Multiscale Approach to the Mechanical Behavior of Epoxy Impregnated Nb3Sn Coils for the 11 T Dipole," in *IEEE Transactions on Applied Superconductivity*, vol. 28, no. 3, pp. 1-6, (2018), 4007706